Electronic Supplementary Material (ESI) for Lab on a Chip.
This journal is © The Royal Society of Chemistry 2019

Lab on a Chip

Soft, skin-interfaced microfluidic systems with integrated enzymatic assays for measuring the concentration of ammonia and ethanol in sweat

Sung Bong Kim, Jahyun Koo, Jangryeol Yoon, Aurélie Hourlier-Fargette, Boram Lee, Seongbin Jo, Shulin Chen, Jungil Choi, Yong Suk Oh, Sang Min Won, Alexander J. Aranyosi, Stephen P. Lee, Jeffrey B. Model, Paul V. Braun, Chulhwan Park, Roozbeh Ghaffari, John A. Rogers

Supporting Information #1

Statistical Analysis: Response surface methodology (RSM) was used to investigate the behavior of enzymatic color development for sweat ammonia and alcohol assays. Central composite design (CCD) techniques yielded 28 runs of experimental design with variables such as enzyme loading, reaction temperature, pH, and chloride concentration. The results defined a second-order (quadratic) polynomial equation by regression of the experimental results (Table S1). The second-order modeling equation can be written as following:

$$y = \beta_0 + \sum \beta_i X_i + \sum \beta_{ii} X_i^2 + \sum \beta_{ij} X_i X_j \quad \text{(Eq. S1)}$$

Here, y is the predicted response, X_i and Xj are the input variables, $\beta_0$is the offset term, β_0 is the i^{th} linear coefficient, β_{ii} is the quadratic coefficient, and β_{ii} is the ij^{th} interaction coefficient. Statistical analysis relied on coding variables to normalize the relative numerical scales of the various factors. The coded values were assigned using following equation:

$$x_i = \frac{(X_i - X_0)}{\Delta X} \quad (i = 1, 2, 3, \ldots, j) \quad \text{(Eq. S2)}$$

Where x_i is the coded value of the variable X_i, X_0 is the independent variable of real value at the center point, and ΔX is the step change value. Table S5 shows the assignment of coded values of the experimental (real) values. Design Expert 7.0 (Stat-Ease, Inc., Minneapolis, MN), a statistical software package, enabled overall statistical studies of experimental design of CCD, linear regression, and analysis of variance (ANOVA).

Results of RSM and statistics: Central composite design, a robust RSM model, facilitates experimental design of various significant factors (enzyme loading amount, temperature of reaction, pH, and chloride concentration) to yield second-order polynomial equations by linear regression of the resulting data (Design Expert 7.0). The linear regression results for ammonia (y_1) and alcohol (y_2) using the experimental data (initial reaction rate) can be summarized in the following equations;

$$y_1 = 8.45 + 0.57X_1 + 1.18X_2 - 0.072X_3 - 0.30X_4 + 0.31X_1X_2 - 0.0028X_1X_3 - 0.19X_1X_4 - 0.028X_2X_3 + 0.058X_2X_4 + 0.12X_3X_4 - 0.63X_1^2 - 0.70X_2^2 - 0.82X_3^2 - 0.48X_4^2 \quad \text{(Eq. S3)}$$

$$y_2 = 22.88 + 3.02X_1 + 3.07X_2 + 0.21X_3 - 0.96X_4 - 0.12X_1X_2 + 0.94X_1X_3 + 0.74X_1X_4 + 0.48X_2X_3 + 0.10X_2X_4 - 1.14X_3X_4 - 2.12X_1^2 - 3.10X_2^2 - 2.47X_3^2 - 1.03X_4^2 \quad \text{(Eq. S4)}$$

Supporting Information #2

Table S1 Fitting results of Lineweaver-Burk plot and the kinetics parameters

a. NH_3

		12	**10**	**8**	**6**	**4**
$1/V_{max}$	(Intercept)	1.592857	1.716812	1.838416	1.658628	1.62157
K_m/V_{max}	(Slope)	16.72805	18.14555	20.09868	23.12009	27.30026
R^2		0.999718	0.999981	0.999908	0.999304	0.99953
V_{max}	($mmol \cdot L^{-1} \cdot min^{-1}$)	0.627803	0.582475	0.543946	0.602908	0.616686
K_m	($mmol \cdot L^{-1}$)	10.50191	10.56933	10.93261	13.93929	16.8357

b. EtOH

		25	**20**	**15**	**10**	**5**
$1/V_{max}$	(Intercept)	0.885042	0.93228	0.905732	0.99461	0.583175
K_m/V_{max}	(Slope)	6.293456	7.57048	9.36009	11.64613	17.53888
R^2		0.99977	0.999348	0.997904	0.9981	0.976902
V_{max}	($mmol \cdot L^{-1} \cdot min^{-1}$)	1.12989	1.072639	1.104079	1.005419	1.714752
K_m	($mmol \cdot L^{-1}$)	7.110916	8.120391	10.33428	11.70925	30.07483

Table S2 Experimental design of CCD and results.

Run	Enzyme loading X_1	Temp. X_2	pH X_3	Cl X_4	Initial Reaction Rate	Enzyme loading X_1	Temp. X_2	pH X_3	Cl X_4	Initial Reaction Rate
1	1	-1	1	-1	0.415	-1	1	1	1	1.400
2	0	0	0	-2	0.798	2	0	0	0	2.584
3	-1	1	1	1	0.620	0	0	0	-2	2.370
4	0	0	0	0	0.806	-1	-1	1	-1	0.944
5	0	0	2	0	0.519	-1	1	-1	1	1.365
6	1	-1	1	1	0.411	1	1	-1	1	1.666
7	0	0	-2	0	0.571	1	-1	-1	-1	0.698
8	1	1	-1	1	0.661	1	1	1	1	1.658
9	0	0	0	2	0.565	1	1	1	-1	2.351
10	-1	1	1	-1	0.587	0	0	0	0	2.115
11	-1	-1	-1	1	0.403	-1	1	1	-1	1.410
12	0	0	0	0	0.941	0	0	0	2	1.805
13	-1	1	-1	1	0.698	0	2	0	0	2.001
14	-1	-1	1	1	0.469	-1	-1	-1	1	0.494
15	-1	-1	1	-1	0.485	-1	1	-1	-1	1.335
16	-1	1	-1	-1	0.633	-2	0	0	0	0.715
17	0	2	0	0	0.814	1	1	-1	-1	1.501
18	1	-1	-1	-1	0.514	1	-1	1	-1	1.574
19	1	1	1	-1	0.786	1	-1	-1	1	1.598
20	0	-2	0	0	0.368	0	0	0	0	2.468
21	-1	-1	-1	-1	0.461	0	0	0	0	2.290
22	0	0	0	0	0.837	0	0	-2	0	1.668
23	2	0	0	0	0.869	0	-2	0	0	0.514
24	1	-1	-1	1	0.415	-1	-1	-1	-1	1.265
25	-2	0	0	0	0.368	-1	-1	1	1	0.515
26	1	1	-1	-1	0.794	0	0	0	0	2.278
27	1	1	1	1	0.735	0	0	2	0	1.351
28	0	0	0	0	0.794	1	-1	1	1	1.200

Table S3 Coded values for RSM.

Factors	(Unit)	Symbol		-2	-1	0	1	2
Enzyme loading	**(%)**	**X1**	NH_3	4	8	12	16	20
	(mg/mL)		EtOH	10	20	30	40	60
Temperature	**(°C)**	**X2**		20	25	30	35	40
pH		**X3**		5	6	7	8	9
Chloride	**(mM)**	**X4**		10	40	70	100	130

Table S4 Fitting results

a. NH_3

Source	Sum of Squares	DF	Mean Square	F-Value	Prob > F
Mean vs Total	6648.46	1	6648.46		
Linear vs Mean	468.6802	4	117.1701	4.763589	0.0060
2FI vs Linear	47.98079	6	7.996799	0.26257	0.9469
Quadratic vs 2FI	333.1909	4	83.29772	5.86732	0.0063
Cubic vs Quadratic	121.4259	8	15.17823	1.20207	0.4385
Residual	63.13374	5	12.62675		
Total	7682.871	28	274.3883		

b. EtOH

Source	Sum of Squares	DF	Mean Square	F-Value	Prob > F
Mean vs Total	1075.241	1	1075.241		
Linear vs Mean	43.74645	4	10.93661	6.542068	0.0011
2FI vs Linear	2.454738	6	0.409123	0.193223	0.9744
Quadratic vs 2FI	25.6222	4	6.40555	8.027783	0.0017
Cubic vs Quadratic	8.101563	8	1.012695	2.2292	0.1963
Residual	2.271433	5	0.454287		
Total	1157.438	28	41.33707		

Table S5 ANOVA

a. NH_3

Source	Sum of Squares	DF	Mean Square	F-value	Prob > F
Model	71.82339	14	5.130242	6.429497	0.0009
X_1	7.914314	1	7.914314	9.918647	0.0077
X_2	33.48371	1	33.48371	41.9636	< 0.0001
X_3	0.125571	1	0.125571	0.157372	0.6980
X_4	2.222851	1	2.222851	2.785797	0.1190
X_1X_2	1.567504	1	1.567504	1.964481	0.1845
X_1X_3	0.000132	1	0.000132	0.000166	0.9899
X_1X_4	0.604506	1	0.604506	0.7576	0.3999
X_2X_3	0.012544	1	0.012544	0.015721	0.9021
X_2X_4	0.053361	1	0.053361	0.066875	0.8000
X_3X_4	0.21669	1	0.21669	0.271568	0.6110
X_1^2	9.620334	1	9.620334	12.05672	0.0041
X_2^2	11.82308	1	11.82308	14.81733	0.0020
X_3^2	16.00993	1	16.00993	20.06452	0.0006
X_4^2	5.437824	1	5.437824	6.814976	0.0216
Residual	10.373	13	0.797923		
Lack of Fit	9.027528	10	0.902753	2.012877	0.3073
Pure Error	1.345467	3	0.448489		
Cor Total	82.19638	27			

Std. Dev.: 0.89, R-square: 0.8738 and CV: 14.41%

b. EtOH

Source	Sum of Squares	DF	Mean Square	F-value	Prob > F
Model	849.85	14	60.704	4.2758	0.0064
X_1	219.14	1	219.14	15.436	0.0017
X_2	226.25	1	226.25	15.937	0.0015
X_3	1.0313	1	1.0313	0.0726	0.7918
X_4	22.259	1	22.259	1.5679	0.2326
X_1X_2	0.2179	1	0.2179	0.0153	0.9033
X_1X_3	14.237	1	14.237	1.0029	0.3349
X_1X_4	8.6804	1	8.6804	0.6114	0.4483
X_2X_3	3.7452	1	3.7452	0.2638	0.6161
X_2X_4	0.1716	1	0.1716	0.0121	0.9141
X_3X_4	20.928	1	20.928	1.4741	0.2463
X_1^2	107.92	1	107.92	7.6019	0.0163
X_2^2	230.76	1	230.76	16.254	0.0014
X_3^2	146.56	1	146.56	10.324	0.0068
X_4^2	25.274	1	25.274	1.7802	0.2050
Residual	184.56	13	14.197		
Lack of Fit	178.32	10	17.832	8.5685	0.0517
Pure Error	6.2432	3	2.0811		
Cor Total	1034.4	27			

Std. Dev.: 3.77, R-square: 0.8216 and CV: 24.45%

Table S6 Results of RSM optimization

Factors	unit	Symbol		Coded	Real
Enzyme loading	**(%) (mg/mL)**	**X1**	NH_3	0.64	14.56
			EtOH	-0.73	22.7
Temperature	**(°C)**	**X2**	NH_3	0.5	32.5
			EtOH	0.6	33
pH		**X3**	NH_3	0.68	7.68
			EtOH	-0.2	6.8
Chloride	**(mM)**	**X4**	NH_3	-0.44	56.8
			EtOH	0.014	70.42

Supporting Information #3

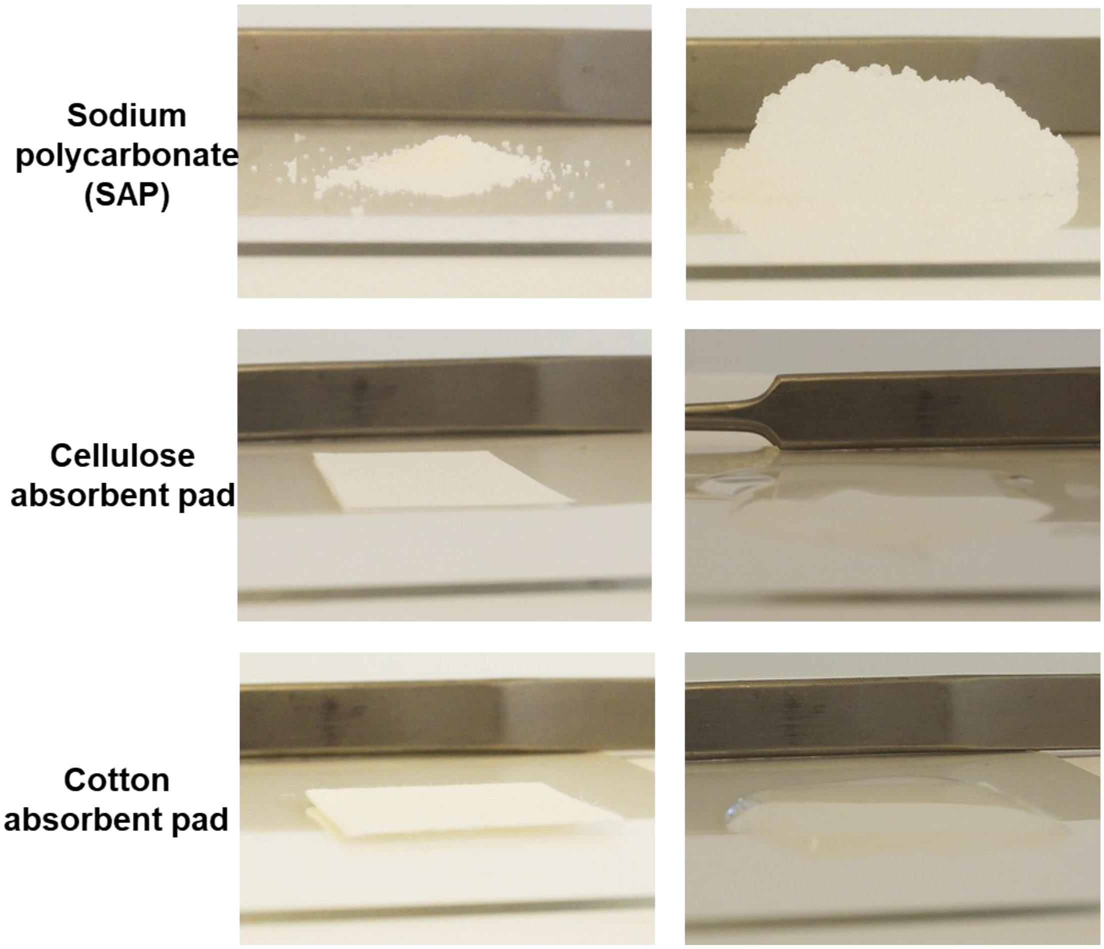

Fig. S1 Super Absorbent Polymer swelling and comparison tests with other absorbent pad of cellulose and cotton. The tests involve same mass of absorbing agent (0.15 g; sodium polycarbonate, cellulose paper, cotton sheet) and dropping 2 mL of distilled water on it.

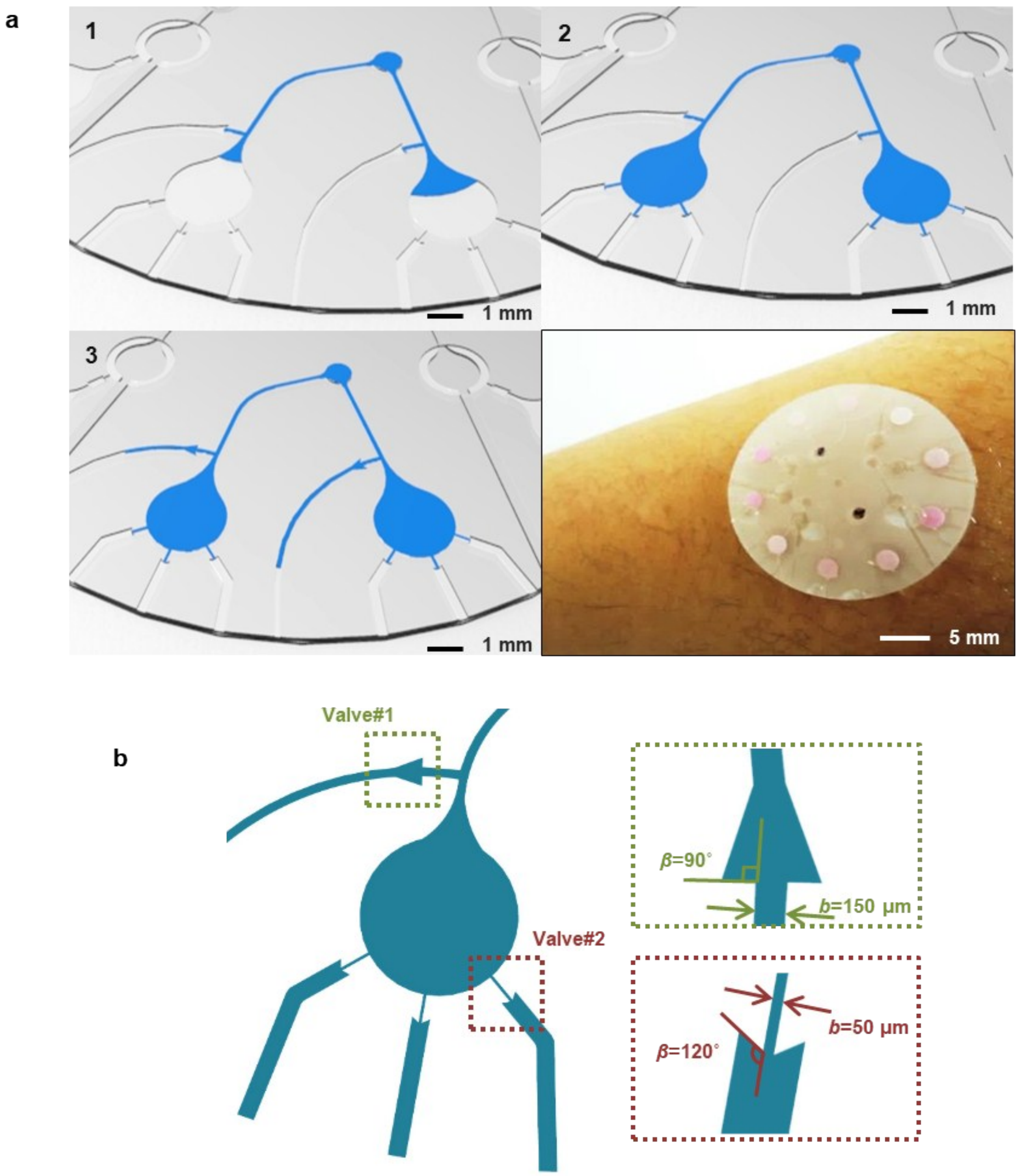

Fig. S2 Schematic drawing of a microfluidic device showing the sweat filling process via capillary burst valves. (a) Cartoons show individual wells filling sequentially. The optical image highlights the appearance of the wells after filling and after reactions are completed. (b) Detailed designs and dimensions of the network of valves.

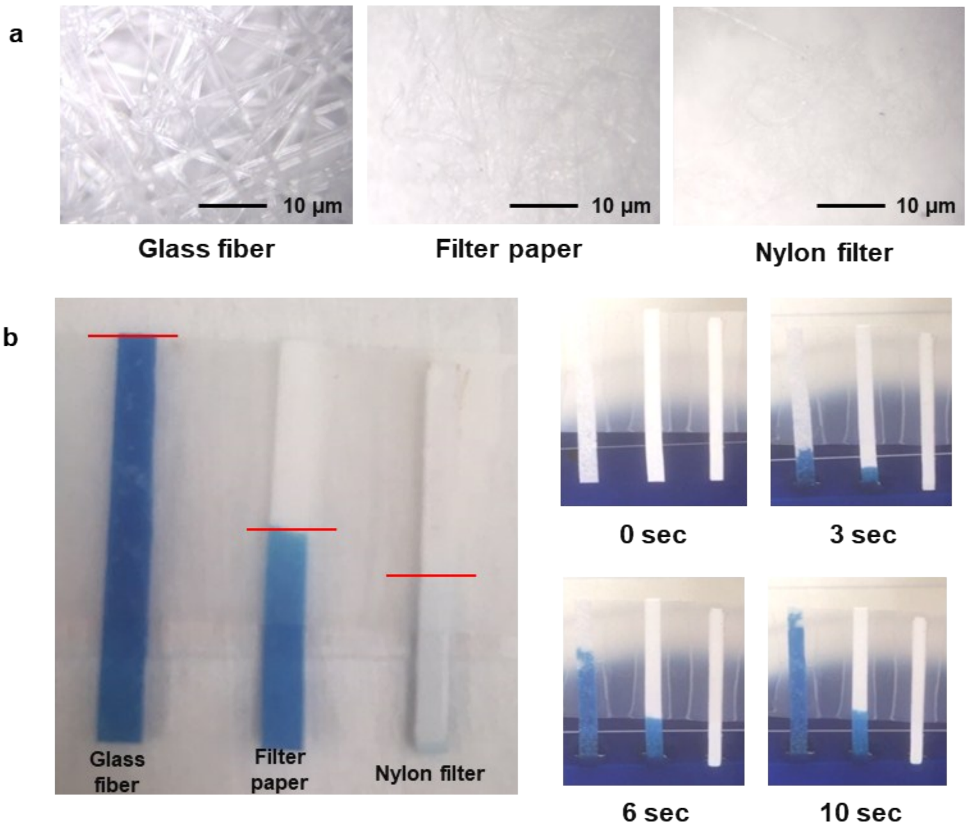

Fig. S3 Enzyme matrix tests. (a) Optical microscope images of glass fiber, filter paper, and nylon filter. (b) Water wetting tests at different time intervals for glass fiber, filter paper, and nylon filter.

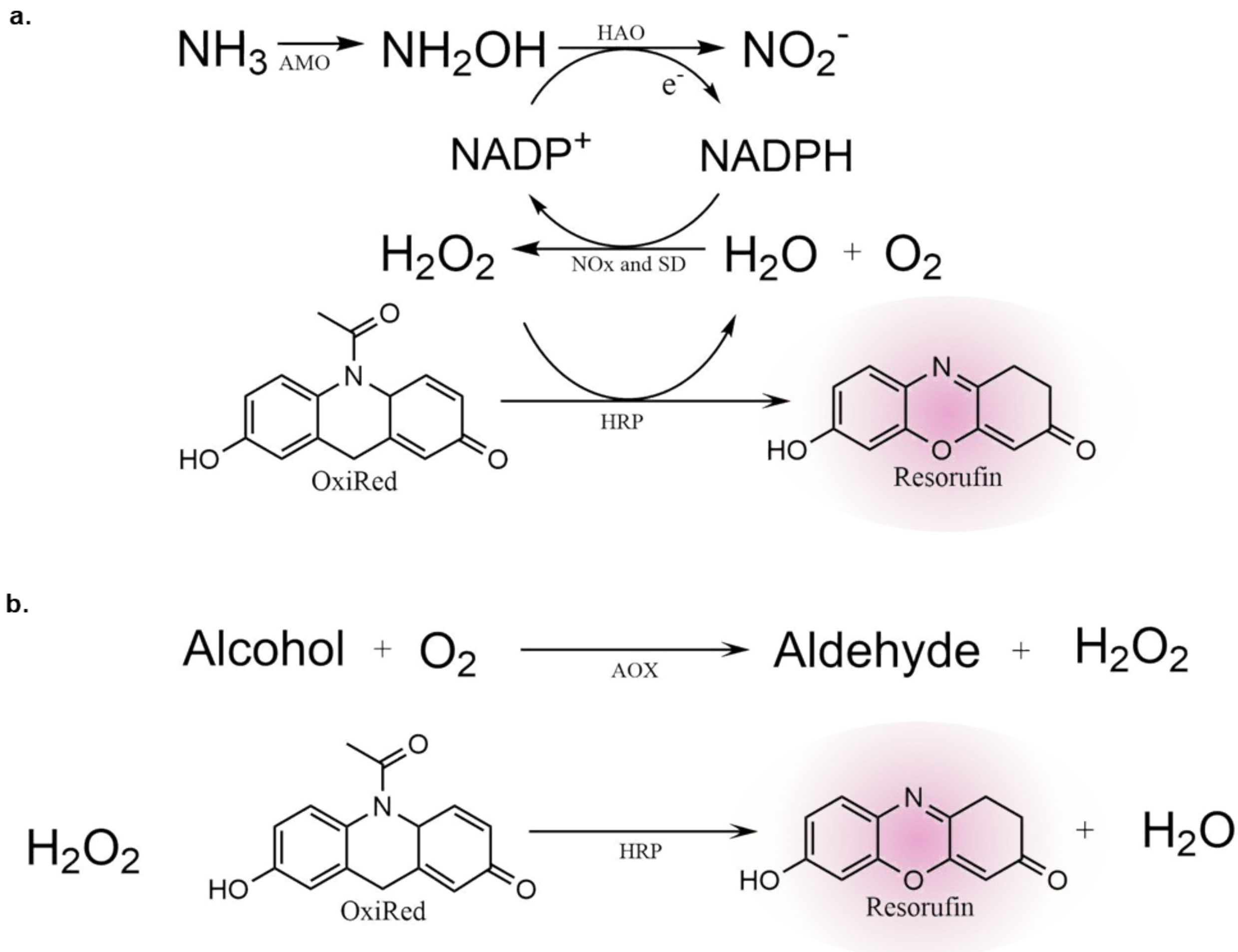

Fig. S4 Reaction formulations for the colorimetric assays. (a) Ammonia oxidation reaction and resorufin production. (b) Alcohol oxidation reaction and resorufin production.

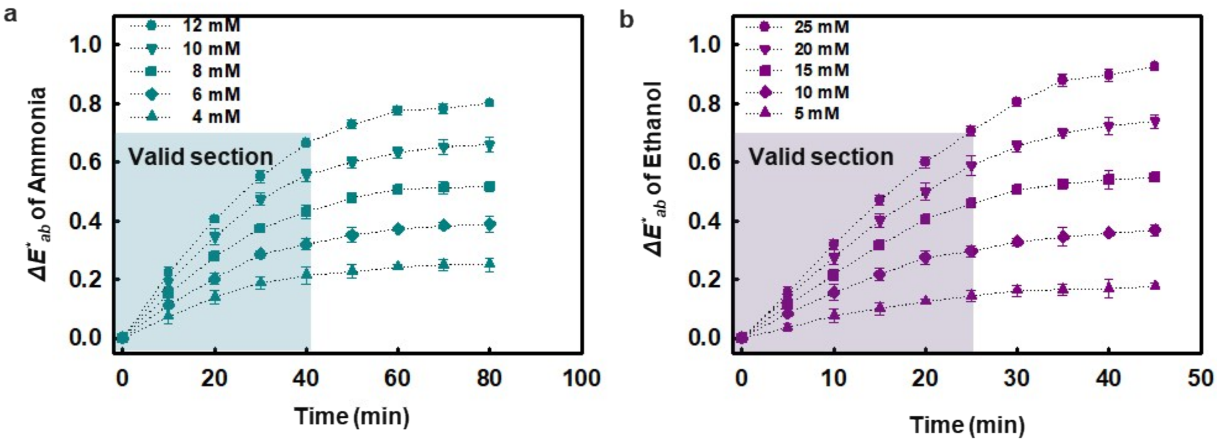

Fig. S5 Color development as a function of time for (a) ammonia and (b) alcohol assays.

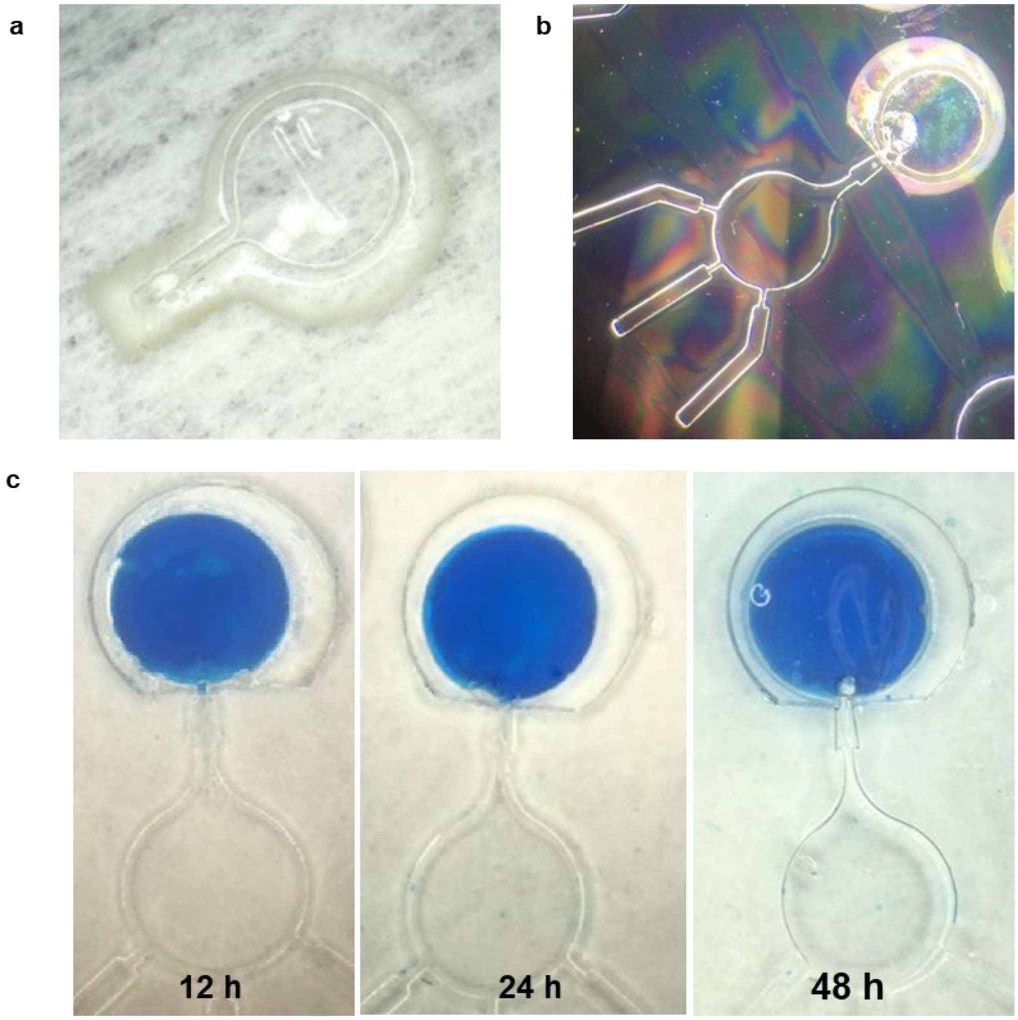

Fig. S6 Prevention of evaporation of pre-loaded reagents using plastic reservoirs. (a) Optical image of the plastic reservoir for liquid reagent pre-loading. (b) Soft lithography of plastic reservoirs. (c) Evaporation tests using pre-loaded reagents in a plastic reservoir monitored over 48 h time period with no significant evaporation effects.

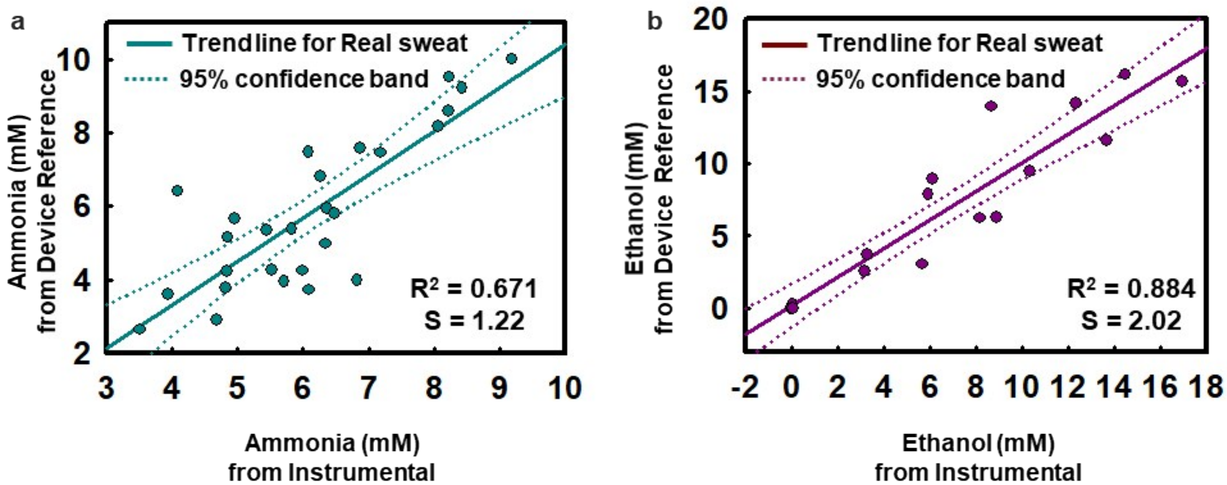

Fig. S7 Comparisons of the results of colorimetric and instrumental assays. (a) Plot of ammonia concentration for a series of human sweat samples that are determined after color analysis and corresponding instrument assay (Liquid chromatography-mass spectrometry system; Waters Synapt G2-Si ESI, MA, USA). (b) Plot of ethanol concentration evaluated in a similar manner.

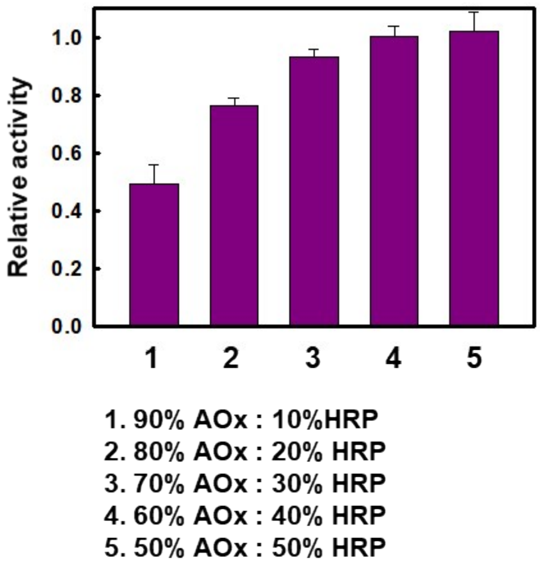

Fig. S8 Effect of AOx-HRP ratio of enzyme cocktail for alcohol assay.

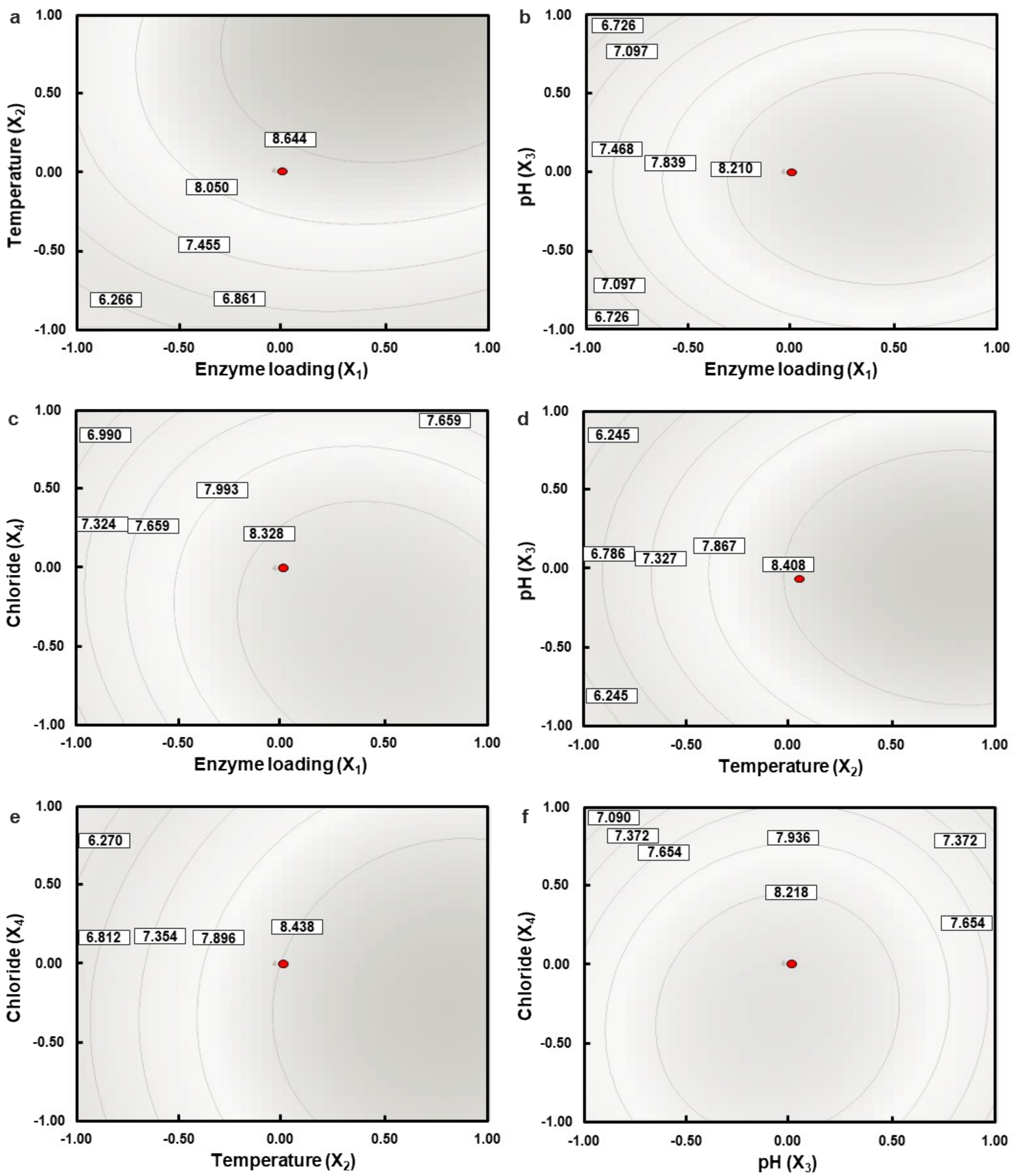

Fig. S9 Contour plots of the response of the ammonia oxidation reaction to external factors. (a) Enzyme loading vs temperature. (b) Enzyme loading vs pH. (c) Enzyme loading vs chloride. (d) Temperature vs pH. (e) Temperature vs chloride. (f) pH vs chloride.

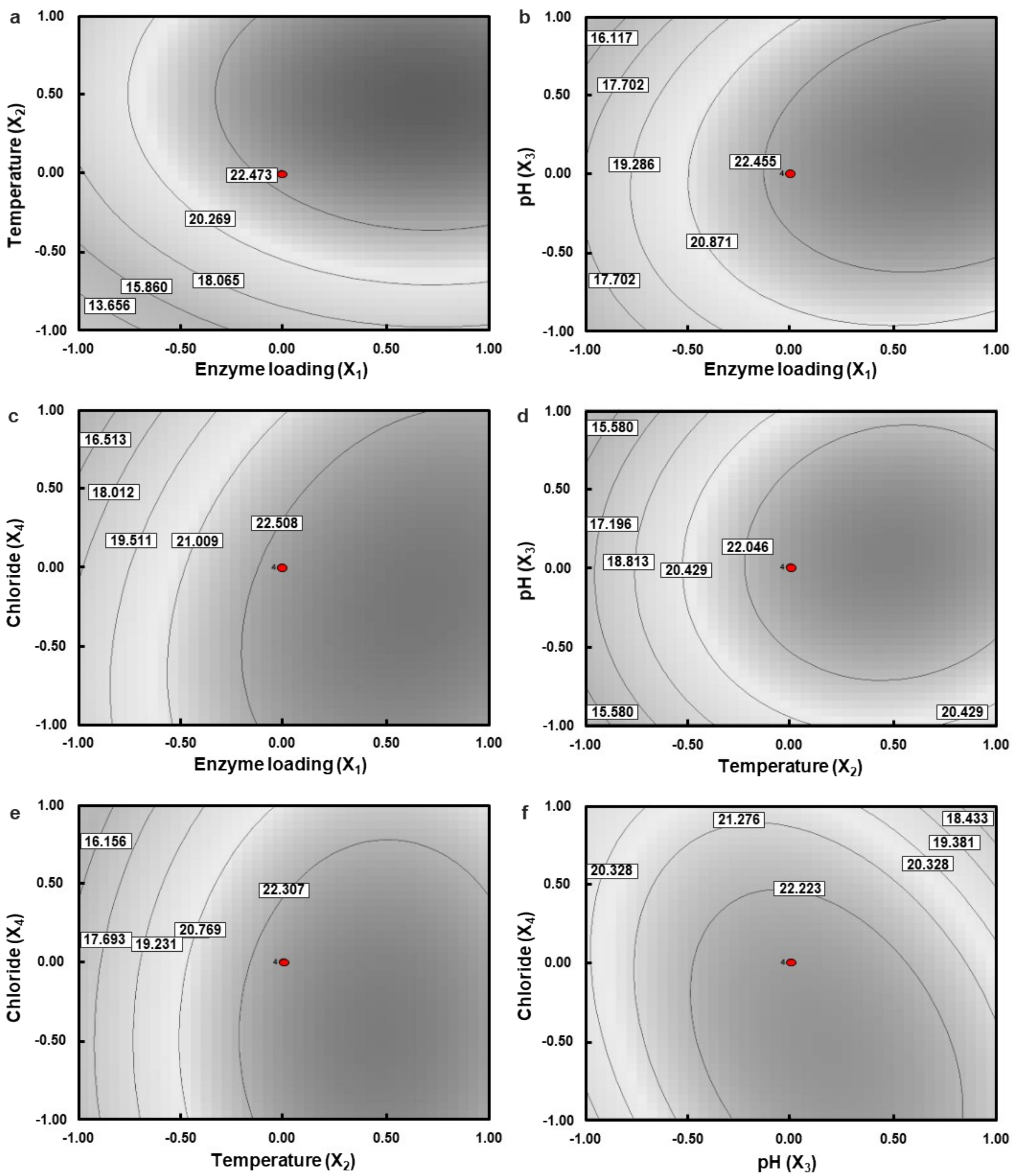

Fig. S10 Contour plots of the response of the alcohol oxidation reaction to external factors. (a) Enzyme loading vs temperature. (b) Enzyme loading vs pH. (c) Enzyme loading vs chloride. (d) Temperature vs pH. (e) Temperature vs chloride. (f) pH vs chloride.

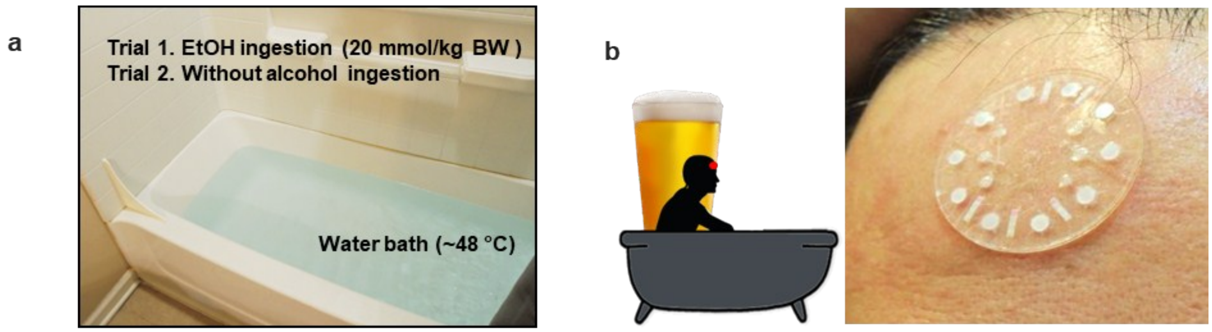

Fig. S11 Field tests conditions with multiple healthy subjects. (a) Optical image of warm water bath prepared for human subjects. (b) Microfluidic device attached to the forehead region on subject.

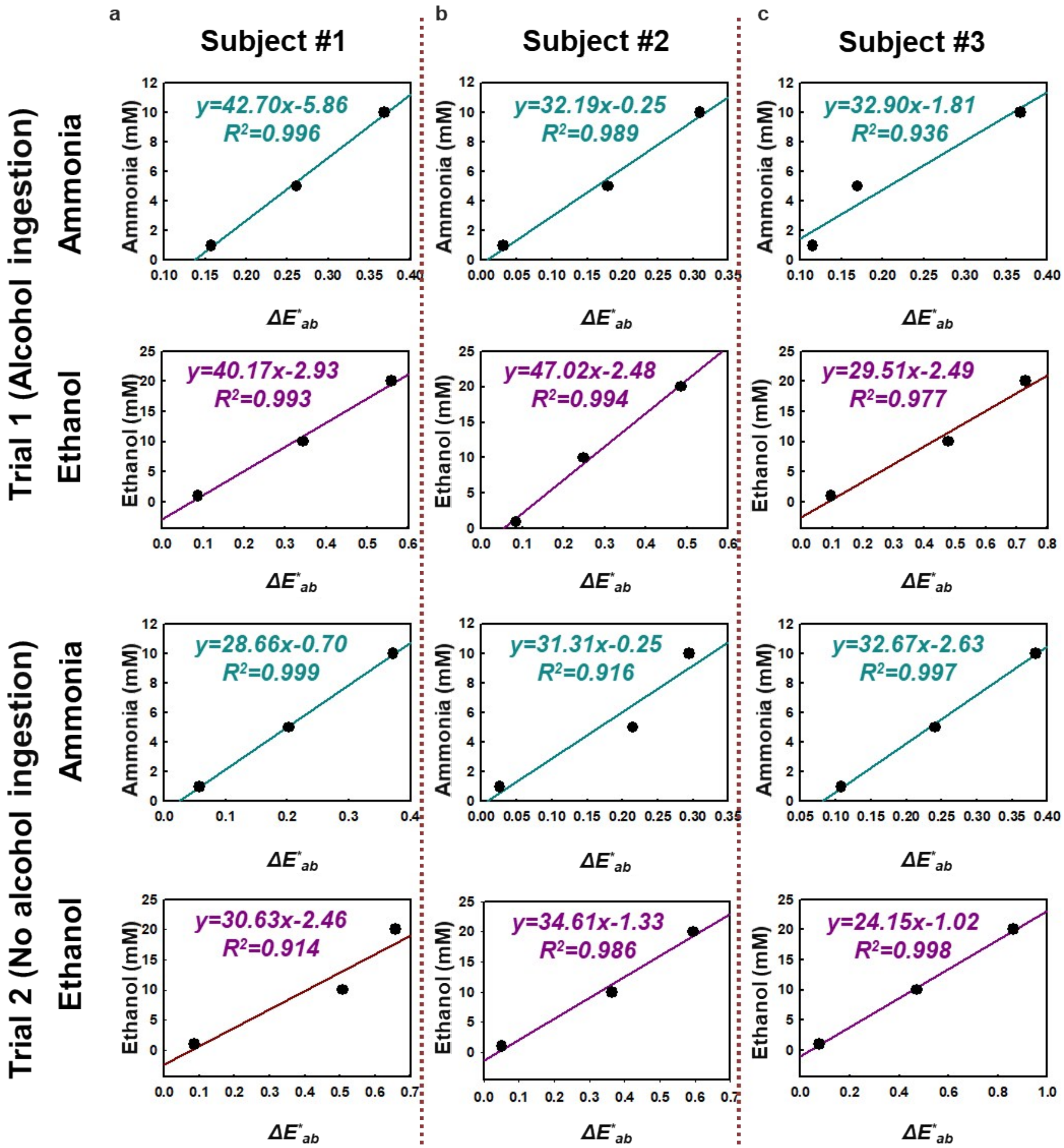

Fig. S12 Calibration curves from reference reaction reservoirs on the devices in field tests for subject #1 (a), subject #2 (b), and subject #3 (c).

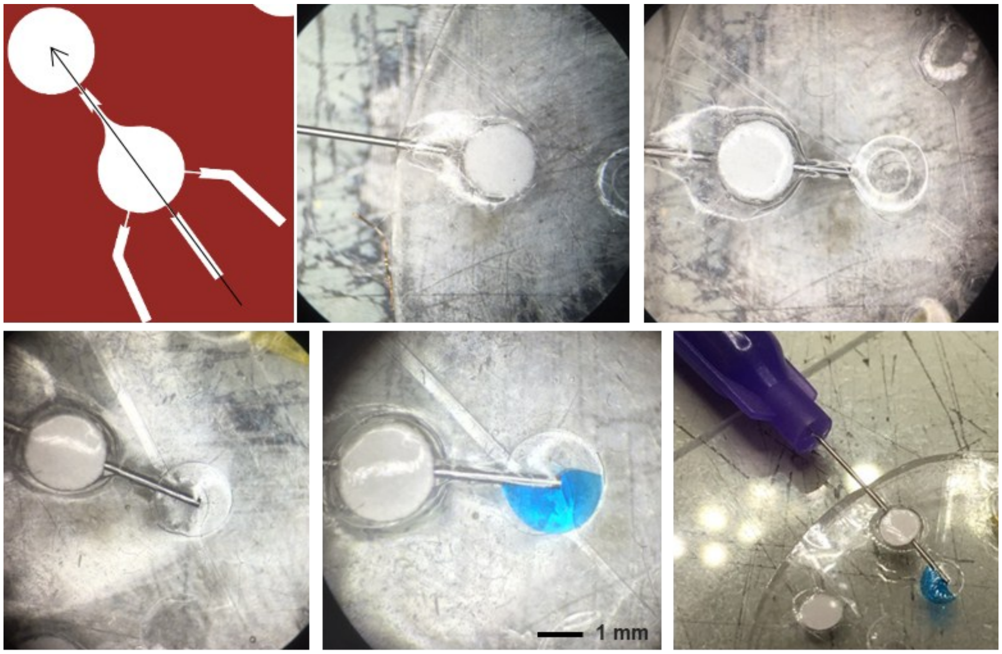

Fig. S13 Reagent pre-loading method using 30 GA (300 μm Φ) needle.